# Chlorination of Reduced Graphene Oxide Enhances the Dielectric Constant of Reduced Graphene Oxide/Polymer Composites

*Jin-Young Kim, Wi Hyoung Lee, Ji Won Suk, Jeffrey R. Potts, Harry Chou, Iskandar N. Kholmanov, Richard D. Piner, Jongho Lee, Deji Akinwande, and Rodney S. Ruoff**

Graphene, a monolayer of carbon atoms arranged into a two-dimensional honeycomb lattice, has attracted tremendous attention owing to its electrical, optical, thermal, and mechanical properties.[1–4] These properties suggest applications that include field-effect transistors, supercapacitors, and sensors, among many others.[5–7] Graphene oxide (G-O) can be chemically reduced to obtain colloidal suspensions of reduced G-O (rG-O) in organic solvents without the use of surfactants.[8–10] Such rG-O suspensions have been studied for many applications, including transparent conducting films and batteries.[11–13]

The dielectric properties of conductor-insulator composites have been previously studied.[14–16] The concentration and aspect ratio(s) of the conducting fillers in these composites, and their spatial distribution, determine the conductor-insulator transition.[14–22] Conductive fillers include metal nanoparticles, carbon nanotubes, carbon black, and carbon fibers.[14–19] The conductor-insulator composites are attracting much attention for potential applications of charge-storage capacitors, thin-film transistors, and antistatic materials owing to their unique properties, i.e., a dramatic increase in dielectric constant in the conductor-insulator composite films near the percolation threshold.[16–18] However, these films have not been used for any practical applications due to issues such as high sintering temperatures (over 1300 °C for metal particles), high dielectric loss, and excessive thickness.[23–25]

Dr. J.-Y. Kim, Dr. W. H. Lee, Dr. J. W. Suk, Dr. J. R. Potts, H. Chou, Dr. I. N. Kholmanov, Dr. R. D. Piner, Prof. R. S. Ruoff
Department of Mechanical Engineering and the Materials Science and Engineering Program
The University of Texas at Austin
Austin, TX 78712, USA
E-mail: r.ruoff@mail.utexas.edu

Prof. W. H. Lee
Department of Organic and Nano System Engineering
Konkuk University
Seoul, 143-701, South Korea

J. Lee, Prof. D. Akinwande
Department of Electrical and Computer Engineering
Microelectronics Research Center
The University of Texas at Austin
Austin, TX 78758, USA

**DOI: 10.1002/adma.201300385**

We present here the dielectric performance of a composite film composed of chlorinated rG-O (hereafter Cl-rG-O) and cyanoethyl pullulan polymer (CEP) as a ferroelectric polymer. We chose the rG-O platelets as conducting fillers because these can be chemically functionalized by a simple process and can be easily dispersed in organic solvents. CEP is a ferroelectric polymer. It has a high dielectric constant among several polymers and can be easily dissolved in *N,N*-dimethylformamide (DMF) solvent. Partial chlorination of rG-O platelets was achieved with chloroform (CF) and separately with chlorobenzene (CB) (see **Figure 1**). The extent of chlorination of rG-O was evaluated by Raman spectroscopy and X-ray photoelectron spectroscopy (XPS). In order to investigate the effect of CF or CB treatment of rG-O platelets on the dielectric performance of the CEP, rG-O/polymer and Cl-rG-O/polymer composite films (less than 2.5 μm thick) were made. The dielectric constant of the composite film containing rG-O gradually increased with increasing rG-O concentration. The composite films were spin-coated and composed of a mixture containing 0.087 wt% rG-O, 81.942 wt% DMF, and 17.971 wt% CEP. The resulting rG-O/polymer films had a dielectric constant of 24, with a dielectric loss of 0.051 at 10 Hz. For Cl-rG-O/polymer composite films, the dielectric constant was 169 (a factor of 5.5 increase compared to rG-O/polymer films) with dielectric loss of 0.05 at 10 Hz. This large enhancement in the dielectric constant is attributed to the interfacial polarization between the Cl-rG-O platelets and the polymer, along with the polar and polarizable C–Cl bonds.

Figure S1a and S1b show atomic force microscopy (AFM) images of the phenyl isocyanate-functionalized rG-O platelets before and after CF treatment. Height profiles were obtained in non-contact mode, as shown in the insets of Figure S1a and S1b, while the step height was measured from the surface of the substrate to the rG-O sheet (Nanotec Electronica, WSxM 5.0 software).[26] The step height of the rG-O before and after the CF treatment was found to be 0.6 to 0.8 nm (roughly the height of a single-layer rG-O platelet).[9] It is difficult to discriminate the thicknesses between the rG-O and Cl-rG-O platelets by an AFM measurement due to the short bonding length (around 2 Å) of C-Cl and the partial chlorination (2 at%).

X-ray photoelectron spectroscopy (XPS) was used to analyze the composition of phenyl isocyanate functionalized rG-O platelets (in the aforementioned spin-coated films) before and after the CF or CB treatment, as shown in **Figure 2**. These XPS spectra were similar to previous XPS spectra on rG-O

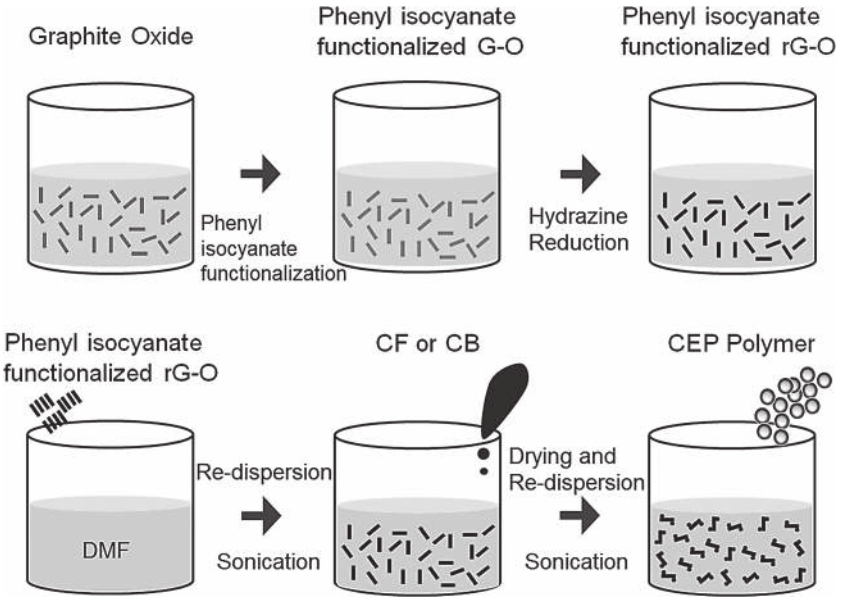


**Figure 1.** The process for producing chemically-reduced (phenyl isocyanate-treated) graphene oxide (rG-O) by hydrazine reduction and the fabrication process for Cl-rG-O/cyanoethyl pullulan polymer composite.

platelets.[27–29] The rG-O treated with CF or CB showed clear Cl 2p peaks, while no Cl 2p peak(s) were detected for the neat rG-O films, as shown in the inset of Figure 2a. Figure 2b–d show the deconvoluted C 1s peaks of rG-O. These components have been attributed to C=C/C–C (284.6 eV), C–N (286.2 eV), C–O/C–O–C (287.4 eV, hydroxyl and epoxy), C=O (288.8 eV, carbonyl), O–C=O (290.3 eV, carboxyl), and $\pi$–$\pi^*$ (291.8 eV) groups.[11,28,30,31] No change in the peak position of the deconvoluted C 1s peak was observed in the XPS spectrum of rG-O platelets before and after the CF or CB treatment. In the case of the rG-O after the CF or CB treatment, the peaks between 286 and 287 eV increased in intensity, perhaps due to the signal from the C-Cl groups (286.5 eV) overlapping with the signal from oxygen-containing groups.[28] Figure 2e,f show the deconvoluted spectra of Cl 2p for rG-O after the CF or CB treatment. Peaks at 200.3 eV and 202 eV were assigned to Cl–C and Cl–C=O groups, respectively, providing evidence that a reaction took place between CF (or CB) and rG-O.[28] These spectra indicated 1.7 and 1.8 at% Cl content after CF or CB treatment, respectively, while no Cl content was detected in the rG-O that was not exposed to CF or CB treatment. From these XPS results, it is thus suggested that Cl atoms or Cl-containing functional groups can be bonded to rG-O by this type of treatment with the CF or CB. Fourier transformed infrared (FTIR) spectra of these samples agreed with the XPS results. As shown in Figure S2 in the Supporting Information, the rG-O treated with CF or CB exhibited a peak at 630 $cm^{-1}$, corresponding to C-Cl stretching, while no peak was detected prior to treatment with CF or CB.

Raman spectroscopy was used to further examine the effect of CF and CB treatment on rG-O, as shown in **Figure 3**a. The Raman spectra of the rG-O and CF or CB treated rG-O samples were all similar. All three had a peak near 1350 $cm^{-1}$ (defect-related D-band), a peak near 1590 $cm^{-1}$ (the G-band originating from in-plane optical vibrations), a peak near 2700 $cm^{-1}$ (the 2D band from a two phonon scattering process), and a peak near 2980 $cm^{-1}$ (due to the D+D' band).[32] The D-band corresponds to the presence of residual oxygen and point defects, as well as the structural disorder induced by tears, wrinkles, and folds in rG-O.[11,33] After CF or CB treatment, the position of the G-band was blue-shifted, while the position of the D-band did not change. This blue shift of the G-band position has been attributed to phonon stiffening with doping of rG-O.[34,35] In Figure 3b, the relationship between the in-plane crystallite size ($L_a$) and the position of the G-band is shown to further illustrate the doping effect by the CF or CB treatment of rG-O. The $L_a$ value, which is used to study the effects of doping, can be assessed by use of the Tuinstra–Koenig relation:

$$L_a(\text{nm}) = \left(2.4 \times 10^{-10}\right) \lambda^4 \left(I_D I_G^{-1}\right)^{-1} \quad (1)$$

where $\lambda$ is the laser wavelength used for Raman measurement and $I_D$ ($I_G$) is the intensity of the D- (G-) band.[36–38] The $L_a$ for Cl-rG-O was lower than that of rG-O, perhaps due to more defects by incorporating Cl atoms on rG-O.[39] This observation, taken together with the detected blue shift in the G-band, implies that the rG-O is doped with Cl by the CF and/or CB treatment. In this system, decomposition of CF of CB during sonication could form, for example, chlorine radicals or chlorine gas that would readily react with rG-O, as shown in **Figure 4**. It has been reported that p-type doping of single-walled carbon nanotubes can be achieved by a similar treatment using organic solvents, such as *o*-CB and CF.[40] As one test of the role of sonication, rG-O was simply dispersed in CF or CB without sonication and spin-coated onto a $SiO_2$(300 nm)-Si wafer, and XPS and Raman spectra of the resulting rG-O samples were collected. All rG-O samples showed clear C 1s, N 1s, and O 1s peaks, as shown in Figure S3a in the Supporting Information. However, Cl 2p peaks were not detected (see Supporting Information, Figure S3b). In the case of Raman analysis, these spectra had peaks at 1356, 1590, and 2700 $cm^{-1}$ with no change in the position of the G- (2D-) band compared to 'neat' rG-O samples, as shown in Figure S4 in the Supporting Information, suggesting that sonication helps drive the reaction of CF or CB with the rG-O platelets.

In addition, the dispersions were found to be stable and homogeneous. As shown in Figure S5a in the Supporting Information, the Tyndall effect was observed with a green laser for rG-O platelets dispersed in DMF, thus implying that the rG-O platelets form a stable colloidal suspension in DMF. No rG-O particles were observed to have precipitated from the mixture after two months, as shown in the inset of Figure S5b in the Supporting Information. The Cl-rG-O platelets also are stable in DMF.

Three different types of composite films were fabricated to investigate the effect of CF or CB treatment (with sonication) of rG-O on the dielectric performance of the composites (see **Figure 5**). These included an undoped rG-O/polymer composite film (labeled in the figure as rG-O), a CF-treated rG-O/polymer



*Adv. Mater.* **2013**,
DOI: 10.1002/adma.201300385

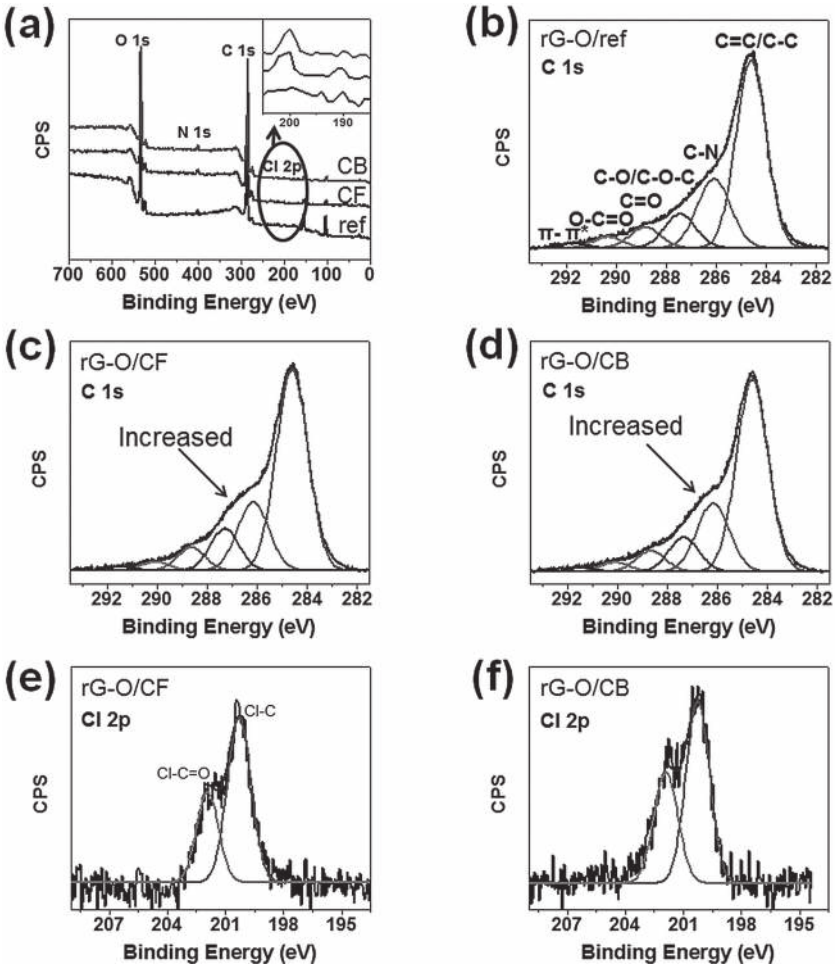


**Figure 2.** a) XPS spectra of the rG-O before and after the CF (or CB) treatment. All of the rG-O samples showed clear C 1s, N 1s, and O 1s peaks. Cl 2p peaks were detected for the rG-O samples after the CF (or CB) treatment. b–d) High-resolution XPS spectra of the C 1s peak for the rG-O: b) before and c,d) after CF (c) or CB (d) treatment. e,f) High-resolution XPS spectra of the Cl 2p peak for rG-O: after CF (e) or CB (f) treatment. Deconvolution revealed the presence of C–Cl (200.3 eV) and Cl–C=O (202 eV) groups.

composite film (rG-O/CF), and a CB-treated rG-O/polymer composite film (rG-O/CB). Each composite film had a thickness of less than 2.5 μm.

The effect of the rG-O concentration in the composite film on dielectric performance at a driving voltage of 0.1 V and a frequency of 1 kHz was studied. Figure 5a,b show the dielectric constant and dielectric loss of the composite films at varying rG-O concentrations up to 1 mg/ml (0.106/99.894 wt%) of rG-O in DMF, which is reported to be the maximum concentration of rG-O that exhibits long-term stability when dispersed in DMF;[9,22] indeed we made a 1.5 mg/ml rG-O/DMF (0.16/99.84 wt%) suspension and the rG-O platelets were found to be partially aggregated after about a day. The dielectric constant of the composite films increased with increasing rG-O concentration, and the dielectric losses were less than 0.035 at 1 kHz. The composite film fabricated using a 1 mg/ml rG-O/DMF suspension exhibited a 21% increase in the dielectric constant (20.3) over the neat polymer film (that had a dielectric constant of 16), with a dielectric loss of 0.034 at 1 kHz. This is likely a result of interfacial polarization: the neighboring rG-O platelets and a thin layer of polymer in between (and/or the rG-O platelets and electrode in between) could form internal barrier layer capacitors (IBLCs). Generally, IBLCs are formed by the conductive fillers with thin dielectric in between; each IBLC contributes a large capacitance.[16,41] An external alternating electric field can induce the migration of electric charge carriers, which generated either by surface plasma resonance or by charge injection from the external electrodes, at the interface between the rG-O platelets and polymer, resulting in differential charge accumulation due to different relaxation times of the two phases. The accumulated charge carriers can induce a polarization, resulting in an increased dielectric constant. Note that none of the composite samples were electrically conducting (i.e., for each sample tested, the loading of rG-O platelets was below the percolation threshold concentration).

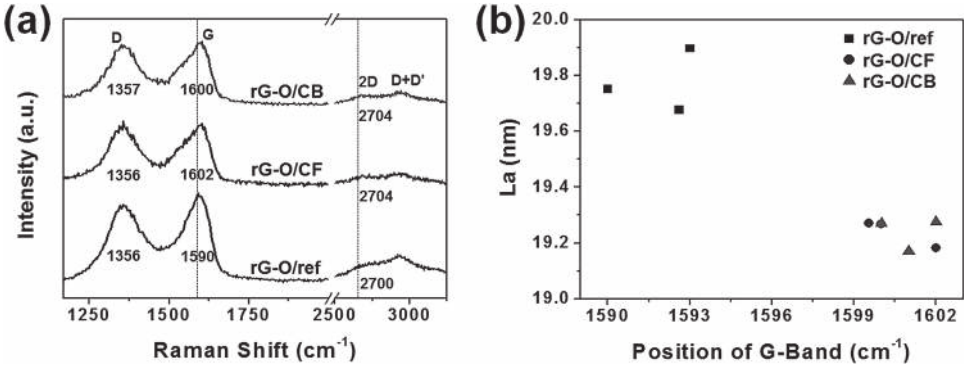


**Figure 3.** a) Raman spectra of the rG-O before and after the CF (or CB) treatment. b) The in-plane crystallite size as a function of the position of G-band for rG-O platelets before and after the CF (or CB) treatment.

ADVANCED MATERIALS
www.advmat.de

Materials Views
www.MaterialsViews.com

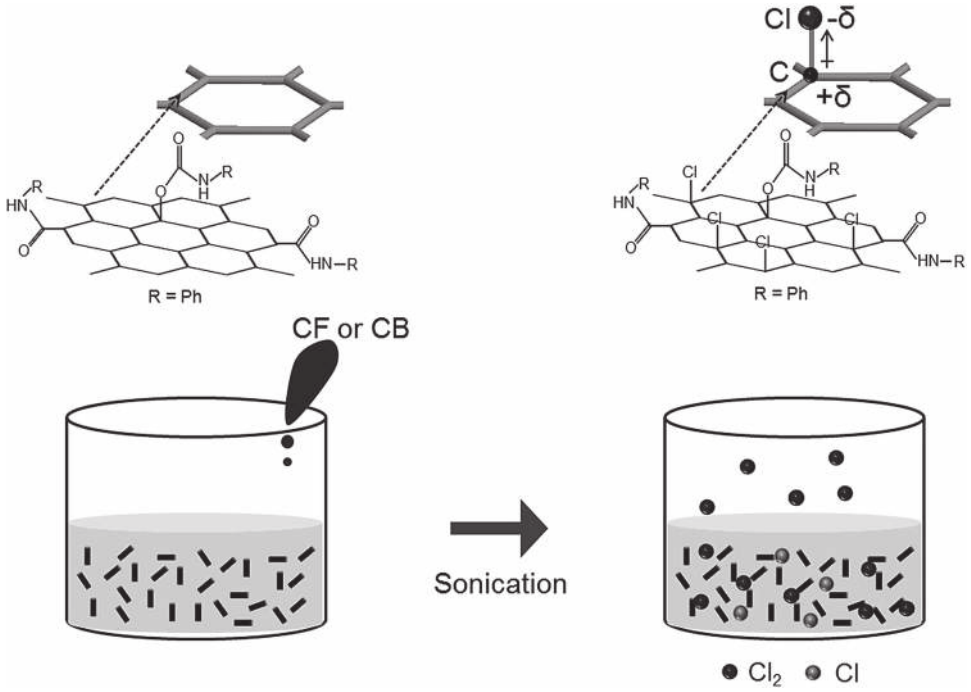


**Figure 4.** Schematic diagrams of proposed reactions during the chlorination of the isocyanate functionalized rG-O platelets where chlorine gas or chlorine radicals would react with rG-O sheets to form C–Cl bonds.

Next, the effect of CF or CB treatment of the rG-O on dielectric performance was investigated. The dielectric performance of the Cl-rG-O composite films was measured at 0.1 V and at frequencies from 10 Hz to 1 MHz, as shown in Figure 5c,d. The dielectric constant of the films decreased slightly with increasing frequency, while the dielectric losses increased.[42]

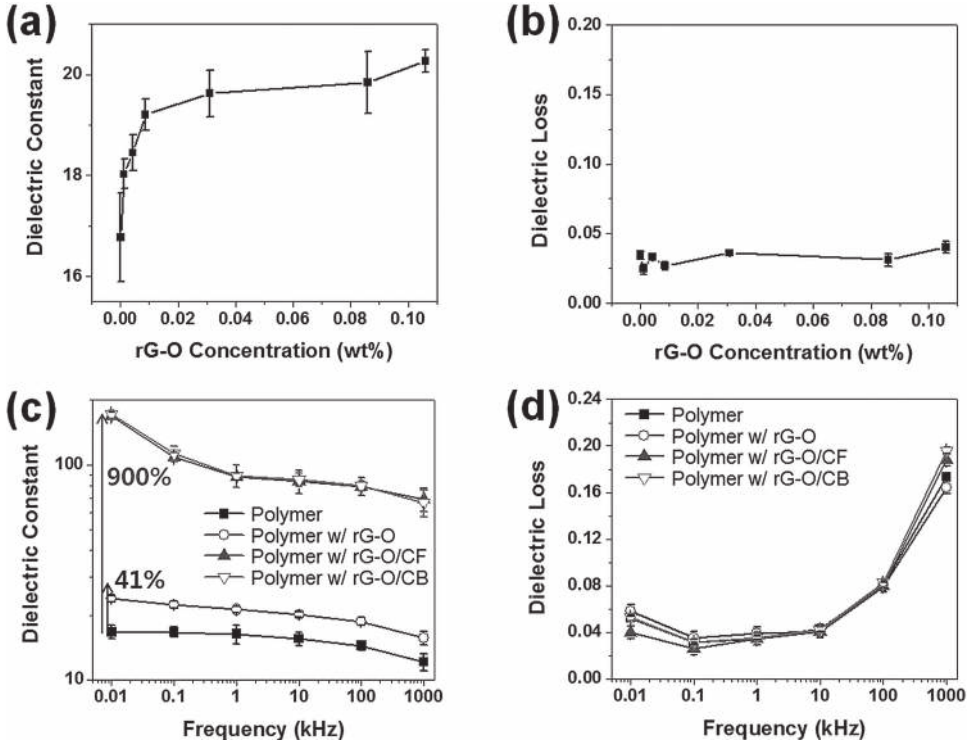


**Figure 5.** a) The dielectric constant and b) dielectric loss of the composite films as a function of rG-O concentration up to 1 mg/ml (0.106/99.894 wt%). c) The dielectric constant and d) dielectric loss of the composite films: neat polymer, rG-O/polymer composite, CF-treated rG-O/polymer composite, and CB-treated rG-O/polymer composite, as a function of applied frequencies ranging from 10 Hz to 1 MHz.



*Adv. Mater.* **2013**,
DOI: 10.1002/adma.201300385

The dielectric constants of the CF- and CB-treated composite films were 169 and 172, respectively, with a dielectric loss of less than 0.05 for both films at 10 Hz, and the dielectric constants of the CF- and CB-treated composite films were 87 and 88.5, respectively, at 1 kHz. At 10 Hz the Cl-rG-O composite had a dielectric constant increased 5.5-fold compared to the untreated rG-O/polymer composite film (dielectric constant of 24). The dielectric constant of the Cl-rG-O/polymer composite film is huge compared to the neat polymer for frequencies less than 1 kHz. The dielectric constant decreases rapidly with increasing frequency until leveling-off at a few hundred Hz (see Supporting Information, Figure S6). This trend is due to interfacial polarization. In general, interfacial polarization can lead to the enhancement of dielectric constant at low frequencies, and can induce a rapid decrease in dielectric constant with increasing frequency.[41,43] At higher frequencies, the polarization can no longer follow rapid changes in the external electric field and relaxation can occur, resulting in a sharp decrease in dielectric constant. The rG-O/polymer composite film shows behavior similar to the Cl-rG-O/polymer composite at low frequency, while the neat polymer film does not. Therefore, interfacial polarization is responsible for the enhanced dielectric constant observed in the Cl-rG-O (or rG-O)/polymer composite film.

We suggest that the mechanism for the large increase in the dielectric constant is as follows. Presuming that C-Cl bonds are present in the Cl-rG-O platelets, the relatively high permanent dipole moment and high polarizability of these bonds could increase the dielectric constant of the composite (see Figure 4). We do not believe that other pairs or groups of atoms contribute significantly to the polarity of the platelets, because the untreated rG-O/polymer films did not exhibit significant increases in the dielectric constant before CF or CB treatment. In addition, the conductivity of the Cl-rG-O (or graphene) sheet was increased, possibly due to a p-type doping effect resulting from the presence of electronegative Cl atoms.[28,44–46] The higher conductivity of the Cl-rG-O platelets may increase the density of the accumulated charge carriers at the interfaces between the Cl-rG-O platelets and the polymer, leading to an increased interfacial polarization[47] that would contribute to an increased dielectric constant. Figure S7 in the Supporting Information shows the relationship between the rG-O or Cl-rG-O (platelets) conductivity and the dielectric constant of the composite films. The electrical resistance of each rG-O sample, prepared by spin-coating of rG-O suspensions without polymer, was measured by the van der Pauw method, and the electrical conductivity was calculated from those measurements. The conductivities of the CF- and CB-treated rG-O platelet films were found to be 1415 and 1488 S/m, respectively, while the untreated rG-O platelet films had a conductivity of 734 S/m. Hence, the dielectric constant of composite films evidently increased with the conductivity of the rG-O platelets, suggesting that interfacial polarization was increased as a result of the CF or CB treatment.

The dielectric strength of the composite films was measured for the neat polymer, polymer with rG-O, polymer with rG-O/CF, and polymer with rG-O/CB. Figure S8 in the Supporting Information shows the leakage current density as a function of applied field. Leakage current density was measured at an applied field of 45 V/μm, since the fluorine-doped tin oxide electrode was seriously damaged for applied fields of more than 45 V/μm. At 45 V/μm, the leakage current densities of the composite films were $8.85 \times 10^{-8}$, $4.15 \times 10^{-7}$, $1.49 \times 10^{-6}$, and $1.50 \times 10^{-6}$ A/cm$^2$ for the neat polymer, polymer with rG-O, rG-O/CF, and rG-O/CB, respectively. The leakage current densities for the composite films of the polymer with rG-O, rG-O/CF, and rG-O/CB were higher than that for the neat polymer film at the same field. This phenomenon can be interpreted through the rG-O platelet interactions that are described below. The rG-O platelets are randomly dispersed in a polymer matrix. While these rG-O platelets are not connected geometrically, they may be connected electrically via tunneling. As previously mentioned, the neighboring rG-O platelets, along with a thin layer of polymer between them, could form IBLCs. When an electric field is applied to the composite film, the thin layer of polymer between rG-O platelets acts as a tunnel barrier. The tunneling of electrons between two adjacent rG-O platelets (conductive fillers) can occur even at relatively low electric field. Therefore, the leakage current density of the composite films with rG-O was higher than that of the neat polymer film. In addition, the high conductivity of the rG-O platelet with CF (CB) treatment can induce yet higher leakage current density, as shown in Figure S8 in the Supporting Information. The leakage current density curves for the composite films with rG-O, rG-O/CF, and rG-O/CB show a sudden increase in the electric field interval of ≈15–17 V/μm. This jump may be because the tunneling barrier was overcome at that electric field.

In conclusion, composite films consisting of CF and CB-treated, phenyl isocyanate-functionalized rG-O and cyanoethyl pullulan polymer were made. Functionalization of the rG-O platelets with Cl atoms and Cl-containing functional groups was achieved by treatment of rG-O/DMF mixtures with CF or CB, as shown by XPS and Raman analysis. The Cl-rG-O platelets showed a 93% increase in conductivity, perhaps due to a p-type doping effect created by Cl atoms. The dielectric constant of the non-chlorinated rG-O/polymer composite film was 24 with a dielectric loss of 0.051. For the case of the Cl-doped rG-O/polymer composite film, the dielectric constant was 169 with a low dielectric loss of 0.050 at 10 Hz. This large increase in dielectric constant was possibly caused by the combination of the polar and polarizable C-Cl bonds and increased interfacial polarization.

## Experimental Section

Figure 1 shows the fabrication process of the rG-O/polymer or Cl-rG-O/polymer composite films. First, phenyl isocyanate-functionalized rG-O was synthesized (details in Supporting Information), then, the phenyl isocyanate-functionalized rG-O was dispersed in DMF using an ultrasonic bath (1 h sonication time), at varying concentrations up to 1 mg/ml (1 mg rG-O/934.4 mg DMF; thus, 0.106/99.894 wt%). Next, CEP was dissolved into the solution, and this mixture was stirred for 12 h. The weight ratio of the polymer to the rG-O/DMF suspension was 18 to 82, which was found to be an appropriate ratio of polymer to rG-O suspension to produce uniform, thin composite films. Based upon the relative concentration of rG-O platelets in the suspension to the polymer, the final loading of rG-O in the composite film was approximately 0.48 wt% (polymer = 99.52 wt%). In the case of the Cl-rG-O/polymer composite film, the rG-O was first dispersed in the DMF at a concentration of 1 mg/ml. Then, 2.7 vol% of CF (or in separate

experiments, 2.7 vol% of CB) was added to the rG-O/DMF suspension and the mixture was treated in an ultrasonic bath for 1 h. Next, 18 wt% CEP was dissolved into the mixture by stirring for 12 h. From these two different mixtures (i.e., CF-treated or CB-treated rG-O), two types of films were made (see Supporting Information, Figure S9a). The dispersions were spun-coat onto fluorine-doped tin oxide (FTO)-coated glass and dried at 130 °C for 30 min. Cr(5 nm)-Au(50 nm) electrodes were then deposited onto the films by thermal evaporation. Figure S9b in the Supporting Information shows a scanning electron microscope (SEM) image of a tilted Cl-rG-O/polymer composite film. The thickness of the composite film was measured by SEM to be 2.5 μm and it had a smooth surface.

The dielectric properties of the composite films on FTO-coated glass were measured with a semiconductor device analyzer (Agilent, B1500A). These measurements were taken at a voltage of 0.1 V and over a range of frequencies. The thicknesses of the composite films were obtained with a Dektak, 6M Stylus Surface Profilometer and the morphology of rG-O (or Cl-rG-O) platelets was examined by AFM (PSIA, XE-100). To evaluate whether the rG-O platelets were chlorinated, samples were examined by Raman spectroscopy (WiTec Alpha, 488 nm laser wavelength) and XPS (Al $K_\alpha$ radiation at 15 kV, 150 W). Films of neat rG-O or of Cl-rG-O were separately prepared by dispersing 1 mg (0.106 wt%) of rG-O (Cl-rG-O) platelets in 1 ml (99.894 wt%) of DMF, and this dispersion was deposited onto a $SiO_2$/Si substrate by spin-coating and then dried at 130 °C for 30 min under air atmosphere. These films were then characterized by Raman, XPS, AFM, and conductivity measurements.

## Supporting Information

Supporting Information is available from the Wiley Online Library or from the author.

## Acknowledgements

We appreciate support from the U.S. Department of Energy (DOE) under award DE-SC0001951.

Received: January 23, 2013
Published online:

[1] Y. Zhu, S. Murali, W. Cai, X. Li, J. W. Suk, J. R. Potts, R. S. Ruoff, *Adv. Mater.* **2010**, *22*, 3906.
[2] D. R. Dreyer, R. S. Ruoff, C. W. Bielawski, *Angew. Chem. Int. Ed.* **2010**, *49*, 9336.
[3] S. Stankovich, D. A. Dikin, G. H. B. Dommett, K. M. Kohlhaas, E. J. Zimney, E. A. Stach, R. D. Piner, S. T. Nguyen, R. S. Ruoff, *Nature* **2006**, *442*, 282.
[4] X. Li, W. Cai, J. An, S. Kim, J. Nah, D. Yang, R. Piner, A. Velamakanni, I. Jung, E. Tutuc, S. K. Banerjee, L. Colombo, R. S. Ruoff, *Science* **2009**, *324*, 1312.
[5] I. Meric, M. Y. Han, A. F. Young, B. Ozyilmaz, P. Kim, K. L. Shepard, *Nat. Nanotechnol.* **2008**, *3*, 654.
[6] C. Liu, Z. Yu, D. Neff, A. Zhamu, B. Z. Jang, *Nano Lett.* **2010**, *10*, 4863.
[7] H. Chang, Z. Sun, K. Y.-F. Ho, X. Tao, F. Yan, W.-M. Kwok, Z. Zheng, *Nanoscale* **2011**, *3*, 258.
[8] C. Gomez-Navarro, R. T. Weitz, A. M. Bittner, M. Scolari, A. Mews, M. Burghard, K. Kern, *Nano Lett.* **2007**, *7*, 3499.
[9] S. Park, J. An, I. Jung, R. D. Piner, S. J. An, X. Li, A. Velamakanni, R. S. Ruoff, *Nano Lett.* **2009**, *9*, 1593.
[10] H. A. Becerril, J. Mao, Z. Liu, R. M. Stoltenberg, Z. Bao, Y. Chen, *ACS Nano* **2008**, *2*, 463.
[11] G. EDA, G. Fanchini, M. Chhowalla, *Nat. Nanotechnol.* **2008**, *3*, 270.
[12] I. N. Kholmanov, M. D. Stoller, J. Edgeworth, W. H. Lee, H. Li, J. Lee, C. Barnhart, J. R. Potts, R. Piner, D. Akinwande, J. E. Barrick, R. S. Ruoff, *ACS Nano* **2012**, *6*, 5157.
[13] X. Zhu, Y. Zhu, S. Murali, M. D. Stoller, R. S. Ruoff, *ACS Nano* **2011**, *5*, 3333.
[14] D. M. Grannan, J. C. Garland, D. B. Tanner, *Phys. Rev. Lett.* **1981**, *46*, 375.
[15] Y. Song, T. W. Noh, S. Lee, J. R. Gaines, *Phys. Rev. B* **1986**, *33*, 904.
[16] C. Pecharroman, J. S. Moya, *Adv. Mater.* **2000**, *12*, 294.
[17] Z.-M. Dang, B. Peng, D. Xie, S.-H. Yao, M.-J. Jiang, J. Bai, *Appl. Phys. Lett.* **2008**, *92*, 112910.
[18] T.-M. Wu, Y.-W. Lim, C.-S. Liao, *Carbon* **2005**, *43*, 734.
[19] Z.-M. Dang, J.-P. Wu, H.-P. Xu, S.-H. Yao, M.-J. Jiang, J. Bai, *Appl. Phys. Lett.* **2007**, *91*, 072912.
[20] M. Moniruzzaman, K. I. Winey, *Macromolecules* **2006**, *39*, 5194.
[21] G. Chen, D. Wu, W. Weng, C. Wu, *Carbon* **2003**, *41*, 579.
[22] J. R. Potts, D. R. Dreyer, C. W. Bielawski, R. S. Ruoff, *Polymer* **2011**, *52*, 5.
[23] C. Pecharroman, F. Esteban-Betegon, J. F. Bartolome, S. Lopez-Esteban, J. S. Moya, *Adv. Mater.* **2001**, *13*, 1541.
[24] Z.-M. Dang, Y.-H. Lin, C.-W. Nan, *Adv. Mater.* **2003**, *15*, 1625.
[25] L. Qi, B. I. Lee, S. Chen, W. D. Samuels, G. J. Exarhos, *Adv. Mater.* **2005**, *17*, 1777.
[26] I. Horcas, R. Fernandez, J. M. Gomez-Rodriguez, J. Colchero, J. Gomez-Herrero, A. M. Baro, *Rev. Sci. Instrum.* **2007**, *78*, 013705.
[27] S. Park, J. An, J. R. Potts, A. Velamakanni, S. Murali, R. S. Ruoff, *Carbon* **2011**, *49*, 3019.
[28] D.-W. Wang, K.-H. Wu, I. R. Gentle, G. Q. Lu, *Carbon* **2012**, *50*, 3333.
[29] C.-Y. Su, Y. Xu, W. Zhang, J. Zhao, X. Tang, C.-H. Tsai, L.-J. Li, *Chem. Mater.* **2009**, *21*, 5674.
[30] S. Dubin, S. Gilje, K. Wang, V. C. Tung, K. Cha, A. S. Hall, J. Farrar, R. Varshneya, Y. Yang, R. B. Kaner, *ACS Nano* **2010**, *4*, 3845.
[31] S. Stankovich, D. A. Dikin, R. D. Piner, K. A. Kohlhaas, A. Kleinhammes, Y. Jia, Y. Wu, S. T. Nguyen, R. S. Ruoff, *Carbon* **2007**, *45*, 1558.
[32] M. Dresselhaus, A. Jorio, M. Hofmann, G. Dresselhaus, R. Saito, *Nano Lett.* **2010**, *10*, 751.
[33] H. C. Schniepp, J.-L. Li, M. J. McAlloster, H. Sai, M. Herrera-Alonso, D. H. Adamson, R. K. Prud'homme, R. Car, D. A. Saville, I. A. Aksay, *J. Phys. Chem. B* **2006**, *110*, 8535.
[34] M. A. Pimenta, G. Dresselhaus, M. S. Dresselhaus, L. G. Cancado, A. Jorio, R. Saito, *Phys. Chem. Chem. Phys.* **2007**, *9*, 1276.
[35] A. Das, S. Pisana, B. Chakraborty, S. Piscanec, S. K. Saha, U. V. Waghmare, K. S. Novoselov, H. R. Krishnamurthy, A. K. Geim, A. C. Ferrari, A. K. Sood, *Nat. Nanotechnol.* **2008**, *3*, 210.
[36] C. Zhang, L. Fu, N. Liu, M. Liu, Y. Wang, Z. Liu, *Adv. Mater.* **2011**, *23*, 1020.
[37] L. S. Panchakarla, K. S. Subrahmanyam, S. K. Saha, A. Govindaraj, H. R. Krishnamurthy, U. V. Waghmare, C. N. R. Rao, *Adv. Mater.* **2009**, *21*, 4726.
[38] L. G. Cancado, K. Takai, T. Enoki, M. Endo, Y. A. Kim, H. Mizusaki, A. Jorio, L. N. Coelho, R. Magalhaes-Paniago, M. A. Pimenta, *Appl. Phys. Lett.* **2006**, *88*, 163106.
[39] H. Wang, T. Maiyalagan, X. Wang, *ACS Catal.* **2012**, *2*, 781.
[40] K. R. Moonoosawmy, P. Kruse, *J. Am. Chem. Soc.* **2008**, *130*, 13417.
[41] C.-W. Nan, Y. Shen, J. Ma, *Annu. Rev. Mater. Res.* **2010**, *40*, 131.
[42] C. Y. Chen, R. J. Birgeneau, M. A. Kastner, N. W. Preyer, T. Thio, *Phys. Rev. B* **1991**, *43*, 392.
[43] M.-J. Jiang, Z.-M. Dang, M. Bozlar, F. Miomandre, J. Bai, *J. Appl. Phys.* **2009**, *106*, 084902.
[44] J. Wu, L. Xie, Y. Li, H. Wang, Y. Ouyang, J. Guo, H. Dai, *J. Am. Chem. Soc.* **2011**, *133*, 19668.
[45] S. Tongay, K. Berke, M. Lemaitre, Z. Nasrollahi, D. B. Tanner, A. F. Hebard, B. R. Appleton, *Nanotechnology* **2011**, *22*, 425701.
[46] K. K. Kim, A. Reina, Y. Shi, H. Park, L.-J. Li, Y. H. Lee, J. Kong, *Nanotechnology* **2010**, *21*, 285205.
[47] Z.-M. Dang, Y.-H. Zhang, S.-C. Tjong, *Synth. Met.* **2004**, *146*, 79.